Density Functional Study of the Oxidative Addition Step in the Carbonylation of Methanol Catalyzed by $[M(CO)_2I_2]^-$ (M = Rh, Ir)

Minserk Cheong*,† and Tom Ziegler‡

Department of Chemistry and Research Institute for Basic Sciences, Kyung Hee University, Seoul 130-701, Korea, and Department of Chemistry, University of Calgary, 2500 University Drive NW, Calgary, Alberta, Canada T2N 1N4

Received August 9, 2004

Quantum mechanical calculations based on density functional theory (DFT) have been carried out on the oxidative addition process $[M(CO)_2I_2]^- + CH_3I \rightarrow [M(CO)_2I_3(CH_3)]^-$ (M = Rh, Ir), which represents an elementary step in methanol carbonylation. The calculated free energies of activation ($\Delta G^{\ddagger}$) in methanol are 19.3 (Ir) and 26.9 kcal mol^{-1} (Rh), respectively, in good agreement with the experimental estimates at 20.9 kcal mol^{-1} (Ir) in dichloromethane and 22.9 kcal mol^{-1} (Rh) in methanol, respectively. The higher barrier for M = Rh is attributed to a relativistic stabilization of the Ir−CH_3 bond. A thermodynamic calculation was carried out on the formation of the intermediate $[M(CO)L_2ICH_3]^{(n-1)-}$ in the general oxidative addition reaction $[M(CO)L_2I]^{n-} + CH_3I \rightarrow [M(CO)L_2ICH_3]^{(n-1)-} + I^-$ (n = 0 or 1) (where L_2 = (CO)I$^-$, $(CO)_2$, or (CO)(MeOH) for M = Ir and L_2 = (CO)I$^-$, *trans*-$(PEt_3)_2$, $Ph_2PCH_2CH_2PPh_2$, $Ph_2PCH_2P(S)Ph_2$, or *S,P*-$SC_2B_{10}H_{10}PPh_2^-$ for M = Rh). The thermodynamic energy difference between the intermediate $[M(CO)L_2ICH_3]^{(n-1)-}$ and the ground state follows the order *S,P*-$SC_2B_{10}H_{10}PPh_2^-$ < *trans*-$(PEt_3)_2$ < $Ph_2PCH_2P(S)Ph_2$ < $Ph_2PCH_2CH_2PPh_2$ < (CO)I$^-$ < $(CO)_2$ in solution with respect to the ligand L_2. This order is to a first approximation determined by the ability of L to stabilize the M−CH_3 bond being formed and the ability of the solvent to stabilize the intermediate $[M(CO)L_2ICH_3]^{(n-1)-}$ relative to ground state. This order agrees well with the experimental kinetic trend.

Introduction

In the late 1960s, workers at Monsanto developed an efficient industrial process for the production of acetic acid. The Monsanto process is based on the carbonylation of methanol by a homogeneous iodide-promoted rhodium catalyst.[1,2] Typical commercial operating conditions are 150−200 °C and 30−100 atm, giving selectivities exceeding 99% based on methanol. A substantial proportion of the 5 million tons of acetic acid made annually uses this process, and the industrial carbonylation of methyl acetate to acetic anhydride also now employs a similar technology.[3−7] The suggested mechanism for the Monsanto process at high iodide concentrations is illustrated[8a,b] in Scheme 1. For the rhodium-based catalyst the oxidative addition of CH_3I to $[Rh(CO)_2I_2]^-$ (**1-[Rh]** of Scheme 1) is rate determining, whereas the migratory insertion step $[Rh(CO)_2I_3(CH_3)]^-$ (**2-[Rh]**) → $[Rh(CO)I_3(COCH_3)]^-$ (**3-[Rh]**) has a lower barrier.[8a,b] The final reductive elimination of CH_3COI from $[Rh(CO)_2I_3(COCH_3)]^-$ (**4-[Rh]**) appears to be fast, but its rate has not been measured.

Scheme 1. Proposed Catalytic Cycle for Carbonylation of Methanol

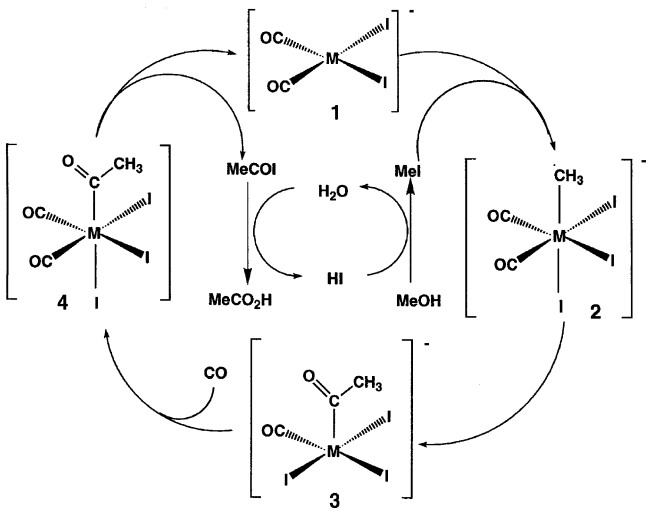

Recently BP Chemicals[6,7] has introduced a new catalytic process in which rhodium is replaced by iridium. The new process, named Cativa, has several advantages over its rhodium-based predecessor, including high reaction rates, good product selectivity, and improved catalyst stability. The carbonylation of metha-

* To whom correspondence should be addressed. E-mail: mcheong@khu.ac.kr.
† Kyung Hee University.
‡ University of Calgary.

(1) Paulik, F. E.; Roth, J. F. *J. Chem. Soc., Chem. Commun.* **1968**, 1578.
(2) Roth, J. F.; Craddock, J. H.; Hershman, A.; Paulik, F. E. *Chem. Technol.* **1971**, 600.
(3) Polichnowski, S. W. *J. Chem. Educ.* **1986**, *63*, 204.
(4) Agreda, V. H. *Chem. Technol.* **1988**, 250.
(5) Zoeller, J. R.; Agreda, V. H.; Cook, S. L.; Lafferty, N. L.; Polichnowski, S. W.; Pond, D. M. *Catal. Today* **1992**, *13*, 73.
(6) *Chem. Br.* **1996**, *32*, 7.
(7) *Chem. Ind. (London)* **1996**, 483.

10.1021/om049383q CCC: $30.25
Publication on Web 05/04/2005

nol catalyzed by rhodium and iridium complexes has been discussed extensively in the literature[9−17] following the pioneering work by Foster.[11,14,15]

Mechanistic studies[8c,18,19] indicate that the iridium system follows the same cycle (Scheme 1) as the rhodium homologue at high iodide concentrations. However oxidative addition of methyl iodide (**1** → **2**) is 100 times faster for iridium than for rhodium, whereas the migratory insertion step (**2** → **3**) is up to 10^6 times slower for the heavier metal.[13,16,17] As a result, the migratory insertion step (**2** → **3**) becomes rate determining in the Cativa process. The difference in relative rates between the two metals is a reflection of the stronger iridium−carbon bond.

Several experimental studies have explored ways in which to reduce the barrier for the rate-determining oxidative addition step (**1** → **2**) of the rhodium system by ligand substitutions.[18,19] We approach here the same objective by conducting a systematic theoretical study on the oxidative addition step (**1** → **2**). Our theoretical investigation explores in the first place the differences between rhodium and iridium in the oxidative addition step involving $[M(CO)_2I_2]^-$ (**2**). We assess next how the thermodyamics of the formation of the intermediate $[M(CO)L_2ICH_3]^{(n-1)-}$ can be changed for rhodium and iridium by substituting the iodide or carbonyl ligand, $L_2 = (CO)I^-$, with other ligands, $L_2 = trans\text{-}(PEt_3)_2$, $Ph_2PCH_2CH_2PPh_2$, $Ph_2PCH_2P(S)Ph_2$, or $S,P\text{-}SC_2B_{10}H_{10}PPh_2^-$, $(CO)_2$, or (CO)(MeOH). These ligands were specifically chosen to compare calculated thermodynamic results with kinetic experimental results using a linear free energy relationship. A theoretical study on the catalytic cycle has appeared recently.[8d,f−i] Since it is difficult to model the S_N2-type reaction especially when appreciable dissociation of the leaving group occurs in the transition state, most of the previous work tends to predict an earlier transition state than the real system. Therefore, in this work we incorporated the solvent effect in each SCF cycle using the conductor-like screening model (COSMO) of Klamt and Schüürmann, which has been recently implemented into the ADF package, to model the S_N2-type reaction more realistically. This approach made it possible to pull the iodide from the methyl far enough to model the real system more closely. As the authors in the previous papers said, the difficulties in modeling S_N2-type reactions lie in the fact that modeling the system becomes very hard when the leaving group is farther away. We have overcome this difficulty by including the solvent effect in the early stage of the calculation. Therefore, we were able to calculate the system with methyl and iodide distances of more than 6 Å, which was impossible in previous papers. This is to our knowledge the first systematic study of the oxidative addition process for the rhodium- and iridium-based carbonylation of methanol with various ligands implementing solvent effects in each SCF cycle and the first study to propose a simple tool to predict the activity of a catalyst.

Computational Details

Stationary points on the potential energy surface were calculated using the Amsterdam Density Functional (ADF) program, developed by Baerends et al.[20,21] and vectorized by Ravenek.[22] The numerical integration scheme applied for the calculations was developed by te Velde et al.[23,24] The geometry optimization procedure was based on the method due to Versluis and Ziegler.[25] The electronic configurations of the molecular systems were described by double-ζ STO basis sets with polarization functions for the H, B, C, O, and S atoms, while triple-ζ Slater-type basis sets were employed for the P, Rh, I, and Ir atoms.[26,27] The 1s electrons of B, C, and O, the 1s-2p electrons of P and S, the 1s-3d electrons of Rh, the 1s-4p electrons of I, and the 1s-4f electrons of Ir were treated as frozen cores. A set of auxiliary[28] s, p, d, f, and g STO functions, centered on all nuclei, was used in order to fit the molecular density and the Coulomb and exchange potentials in each SCF cycle. Energy differences were calculated by augmenting the local exchange−correlation potential by Vosko et al.[29] with Becke's[30] nonlocal exchange corrections and Perdew's[31] nonlocal correlation corrections (BP86). Geometries were optimized including nonlocal corrections, and the harmonic vibrational frequencies were also computed at this level of theory. Thermodynamic properties were evaluated according to standard textbook procedures.[32] Solvation free energies were calculated in each SCF cycle using the conductor-like screening model (COSMO) of Klamt and Schüürmann,[33] which has been recently implemented into the ADF package.[34] To compare

(8) (a) Haynes, A.; Mann B. E.; Gulliver, D. J.; Morris, G. E.; Maitlis, P. M. *J. Am. Chem. Soc.* **1991**, *113*, 8567. (b) Haynes, A.; Mann, B. E.; Morris, G. E.; Maitlis, P. M. *J. Am. Chem. Soc.* **1993**, *115*, 4093. (c) Ghaffar, T.; Adams, H.; Maitlis, P. M.; Sunley, G. J.; Baker, M. J.; Haynes, A. *Chem. Commun.* **1998**, 1023. (d) Griffin, T. R.; Cook, D. B.; Haynes, A.; Pearson, J. M.; Monti, D.; Morris, G. E. *J. Am. Chem. Soc.* **1996**, *118*, 3029. (e) Fulford. A.; Hickey, C. E.; Maitlis, P. M. *J. Organomet. Chem.* **1990**, *398*, 311. (f) Ivanova, E. A.; Gisdakis, P.; Nasluzov, V. A.; Rubailo, A. I.; Rösch, N. *Organometallics* **2001**, *20*, 1161. (g) Cavallo, L.; Sola, M. *J. Am. Chem. Soc*. **2001**, *12*, 12294. (h) Kinnunen, T.; Laasonen, K. *J. Mol. Struct. (THEOCHEM)* **2001**, *542*, 273. (i) Daura-Oller, E.; Poblet, J. M.; Bo, C. *Dalton Trans*. **2003**, 92.

(9) Brodzki, D.; Denise, B.; Pannetier, G. *J. Mol. Catal.* **1977**, *2*, 149.

(10) Matsumoto, T.; Mizoroki, T.; Ozaki, A. *J. Catal.* **1978**, *51*, 96.

(11) Forster, D. *Adv. Organomet. Chem.* **1979**, *17*, 255.

(12) Dekleva, T. W.; Forster, D. *Adv. Catal.* **1986**, *34*, 81.

(13) Maitlis, P. M.; Haynes, A.; Sunley, G. J.; Howard, M. J. *J. Chem. Soc., Dalton Trans.* **1996**, 2187.

(14) Forster, D. *J. Chem. Soc., Dalton Trans.* **1979**, 1639.

(15) Forster, D.; Singleton, T. C. *J. Mol. Catal.* **1982**, *17*, 299.

(16) Ellis, P. R.; Pearson, J. M.; Haynes, A.; Adams, H.; Bailey, N. A.; Maitlis, P. M. *Organometallics* **1994**, *13*, 3215.

(17) Bassetti, M.; Monti, D.; Haynes, A.; Pearson, J. M.; Stanbridge, I. A.; Maitlis, P. M. *Gazz. Chim. Ital.* **1992**, *122*, 391.

(18) (a) Rankin, J.; Poole, A. D.; Benyei, A. C.; Cole-Hamilton, D. J. *J. Chem. Soc., Chem. Commun.* **1997**, 1835. (b) Lee, H.-S.; Bae, J.-Y.; Kim, D.-H.; Kim, H. S.; Kim, S.-J.; Cho, S.; Ko, J.; Kang, S. O. *Organometallics* **2002**, *21*, 210.

(19) Gonsalvi. L.; Adams, H.; Sunley, G. J.; Ditzel, E.; Haynes, A. *J. Am. Chem. Soc.* **1999**, *121*, 11233.

(20) Baerends, E. J.; Ellis, D. E.; Ros, P. *Chem. Phys.* **1973**, *2*, 41.

(21) Baerends, E. J.; Ros, P. *Chem. Phys.* **1973**, *2*, 52.

(22) Ravenek, W. *Algorithms and Applications on Vector and Parallel Computers*; te Riele, H. J. J., Dekker, T. J., van de Horst, H. A., Eds.; Elsevier: Amsterdam, The Netherlands, 1987.

(23) te Velde, G.; Baerends, E. J. *J. Comput. Chem.* **1992**, *99*, 84.

(24) Boerrigter, P. M.; te Velde, G.; Baerends, E. J. *Int. J. Quantum Chem.* **1988**, *33*, 87.

(25) Versluis, L.; Ziegler, T. *J. Chem. Phys.* **1988**, *88*, 322.

(26) Snijders, J. G.; Baerends, E. J.; Vernoijs, P. *At. Nucl. Data Tables* **1982**, *26*, 483.

(27) Vernoijis, P.; Snijders, J. G.; Baerends, E. J. *Slater Type Basis Functions for the Whole Periodic System*; Internal Report (in Dutch); Department of Theoretical Chemistry, Free University: Amsterdam, The Netherlands, 1981.

(28) Krijn, J.; Baerends, E. J. *Fit Functions in the HFS Method*; Internal Report (in Dutch); Department of Theoretical Chemistry, Free University: Amsterdam, The Netherlands, 1984.

(29) Vosko, S. H.; Wilk, L.; Nusair, M. *Can. J. Phys.* **1980**, *58*, 1200.

(30) Becke, A. *Phys. Rev. A* **1988**, *38*, 3098.

(31) (a) Perdew, J. P. *Phys. Rev. B* **1986**, *34*, 7406. (b) Perdew, J. P. *Phys. Rev. B* **1986**, *33*, 8822.

(32) McQuarrie, D. A. *Statistical Thermodynamics*; Harper & Row: New York, 1973.

(33) Klamt, A.; Schüürmann, G. *J. Chem. Soc., Perkin Trans. 2* **1993**, 799.

(34) (a) Pye, C. C.; Ziegler, T. *Theor. Chem. Acc.* **1999**, *101*, 396. (b) Margel, P.; et al. To be submitted for publication.

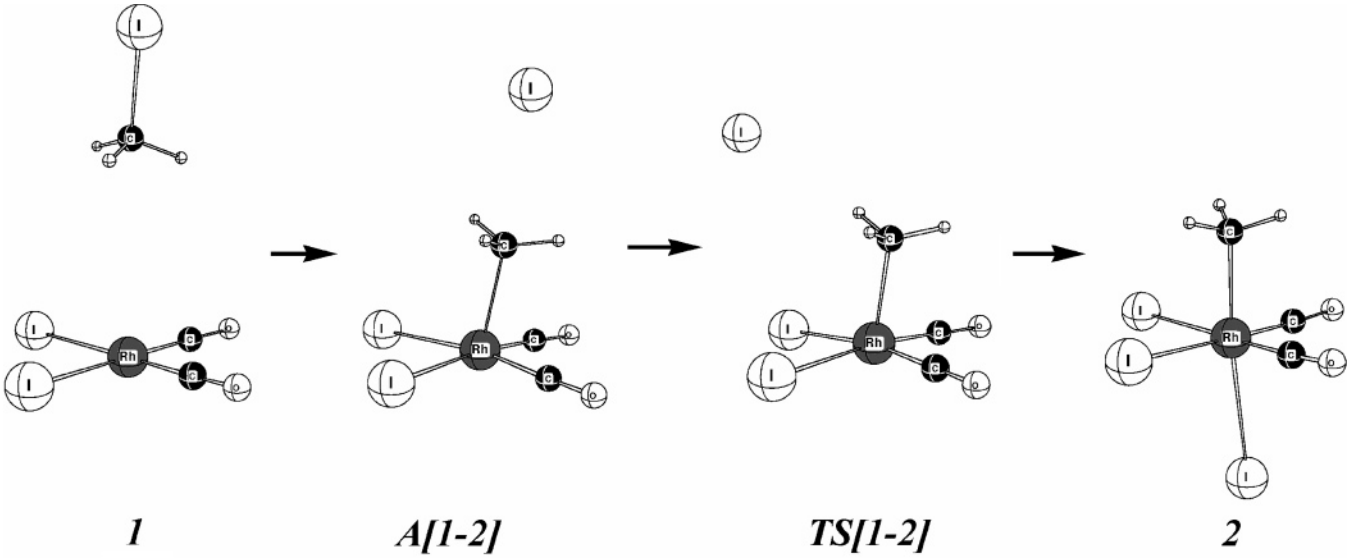

Figure 1. Key structures in the oxidative addition process.

Table 1. Activation Parameters[a] for the Oxidative Addition of Methyl Iodide

	$\Delta S^{\ddagger}$(s) (calc)	$\Delta H^{\ddagger}$(s) (calc)[e]	$\Delta G^{\ddagger}$(s) (calc)[f]	$\Delta S^{\ddagger}$ (expt)[b]	$\Delta H^{\ddagger}$ (expt)[b]	$\Delta G^{\ddagger}$ (expt)[b]	ϵ[g]
cis-$[Rh(CO)_2I_2]^-$	−43.9	13.8	26.9	−28.7[c]	14.3[c]	22.9[c]	32.63
[Rh(dppe)(CO)I]				−39.91[h]	9.56[h]	21.46[h]	9.08
[Rh(dppms)(CO)I]				−34.42[h]	11.23[h]	21.49[h]	9.08
cis-$[Ir(CO)_2I_2]^-$	−44.6	6.0	19.3				32.63
				−27.0[d]	12.9[d]	20.9[d]	9.08

[a] At 298.15 K and 1 atm. All energies are in kcal mol^{-1}, entropies in cal K^{-1} mol^{-1}. Barrier calculated from reactant to **TS[1−2]**. [b] Experimental numbers are obtained in solution. Solvents are MeOH (ϵ = 32.63) or dichloromethane (ϵ = 9.08) for rhodium and dichloromethane (ϵ = 9.08) for iridium. MeOH (ϵ = 32.63) is used in theoretical calculations for both metals. [c] Ref 8e. [d] Ref 16. [e] $\Delta H^{\ddagger}(s) = \Delta H^{\ddagger}(g) + \Delta H^{\ddagger el}(s)$. Here $\Delta H^{el}(s)$ is the electrostatic solvation stabilization (see ref 34) calculated in each SCF cycle. [f] $\Delta G^{\ddagger}(s) = \Delta H^{\ddagger}(s) - T\Delta S^{\ddagger}(s)$. [g] Dielectric constants for the solvents in the experiments. [h] Ref 19.

with experimental results, methanol (ϵ_o = 32.63) was used for iridium and rhodium complexes as a solvent. First-order Pauli scalar relativistic corrections[35,36] were added variationally to the total energy for all systems. In view of the fact that all systems investigated in this work show a large HOMO−LUMO gap, a spin-restricted formalism was used for all calculations. No symmetry constraints were used. The transition states were fully optimized with one imaginary frequency.

Results and Discussion

Our discussion of the oxidative addition process is divided into two parts. The first deals with the generic $[M(CO)_2I_2]^-$ system for M = Rh or Ir. The second part discusses how the thermodynamics of the S_N2 reaction is changed by substituting the I^- or CO ligand by other ligands L_2 in $[Rh(CO)L_2I]$ (where L_2 = *trans*-$(PEt_3)_2$, $Ph_2PCH_2CH_2PPh_2$, $Ph_2PCH_2P(S)Ph_2$, or *S,P*-$SC_2B_{10}H_{10}PPh_2^-$) and in $[Ir(CO)L_2I]$ (where L_2 = $(CO)_2$ or (CO)(MeOH)).

1. Oxidative Addition Involving $[M(CO)_2I_2]^-$ (M = Rh, Ir). We shall first discuss the basic oxidative addition process

$$[M(CO)_2I_2]^- + CH_3I \rightarrow [M(CO)_2I_3(CH_3)]^- \quad (M = Rh, Ir) \quad (1)$$

with an emphasis on the difference between the two metals. The process in eq 1 will be analyzed on the basis of static DFT calculations.

The square-planar d^8 low-spin *cis*-$[M(CO)_2I_2]^-$ catalyst (**1**) (M = Rh, Ir) was preferred over the corresponding *trans*-isomer by 8.2 (Rh) and 15.1 kcal mol^{-1} (Ir), respectively. The energy difference is enhanced slightly in solution (CH_3I) to 8.8 (Rh) and 16.0 kcal mol^{-1} (Ir). The oxidative addition product d^6 low-spin *fac,cis*-$[M(CO)_2I_3(CH_3)]^-$ (**2**) (M = Rh, Ir) from the reaction between CH_3I and $[M(CO)_2I_2]^-$ (**1**) was the most stable conformation for both metals in solution as well as in the gas phase. However, for rhodium the *mer,trans*-isomer is only marginally less stable.[37]

The metal center attacks in the oxidative addition process of eq 1 the methyl group in a S_N2-type fashion. The metal approaches in this process the methyl iodide *trans* to the leaving iodide group, leading to an intermediate adduct, **A[1−2]** (see Figure 1). In this adduct, the metal−methyl bond is under development, whereas the methyl−iodide bond is substantially stretched. The final formation of the M−methyl bond and dissociation of the Me−I bond take place in the transition state **TS[1−2]** (see Figure 1). The energy necessary to break the methyl−iodide bond is partially compensated for by the formation of the metal−methyl linkage.

The calculated free energies of activation ($\Delta G^{\ddagger}$) for the process in eq 1 are 19.3 (Ir) and 26.9 kcal mol^{-1} (Rh) in MeOH solution, as shown in Table 1. These values are in reasonable agreement with the experimental estimates at 20.9 kcal mol^{-1} (Ir)[16] in CH_2Cl_2 and 22.9 kcal mol^{-1} (Rh)[8e] in MeOH, respectively. Thus, our calculations reproduce well the increase in $\Delta G^{\ddagger}$ from

(35) Snijders, J. G.; Baerends, E. J. *Mol. Phys.* **1978**, *36*, 1789.
(36) Snijders, J. G.; Baerends, E. J.; Ros, P. *Mol. Phys.* **1979**, *38*, 1909.
(37) Cheong, M.; Schmid, R.; Ziegler, T. *Organometallics* **2000**, *19*, 1973.

iridium to rhodium. The increase reflects the fact that relativistic effects make the M−CH_3 bond stronger for the heavier metal (iridium).[38]

The agreement between experiment and theory for the individual components $\Delta H^{\ddagger}$ and $\Delta S^{\ddagger}$ to $\Delta G^{\ddagger} = \Delta H^{\ddagger} - T\Delta S^{\ddagger}$ is not as good as for $\Delta G^{\ddagger}$ itself. For rhodium we find $\Delta H^{\ddagger} = 13.8$ kcal mol^{-1} and $\Delta S^{\ddagger} = -43.9$ cal mol^{-1} K^{-1} compared to the experimental estimates[8e] of $\Delta H^{\ddagger} = 14.3$ kcal mol^{-1} and $\Delta S^{\ddagger} = -28.7$ cal mol^{-1} K^{-1}, respectively. A similar situation is found for iridium. Here $\Delta S^{\ddagger}$ is observed[16] to have a small negative value of −27.0 cal mol^{-1} K^{-1} compared to our estimate of −44.6 cal mol^{-1} K^{-1}. On the other hand, experiment[16] finds a large activation enthalpy of $\Delta H^{\ddagger} = 12.9$ kcal mol^{-1} compared to our lower estimate of 6.0 kcal mol^{-1}. We interpret the difference in terms of a strong dependence of both $\Delta H^{\ddagger}$ and $\Delta S^{\ddagger}$ on the solvent. Even though we have incorporated solvent effects in each SCF cycle, we have still not been able to model the real system close enough. The explicit solvent involvement might raise $\Delta H^{\ddagger}$ at the expense of decreasing $-T\Delta S^{\ddagger}$. The result could be a modest decrease in $\Delta G^{\ddagger}$ and much larger (compensating) changes in the components $\Delta H^{\ddagger}$ and $\Delta S^{\ddagger}$. Large compensating variations in $\Delta H^{\ddagger}$ and $\Delta S^{\ddagger}$ due to changes in external parameters such as solvent polarity have been termed an isokinetic response.[39,40]

Experimental results for rhodium demonstrate the point made above. Thus, by changing the solvent from methanol ($\epsilon = 32.63$) to dichloromethane ($\epsilon = 9.08$), methyl iodide ($\epsilon = 7.00$), or methyl acetate ($\epsilon = 6.68$) considerable changes are observed in $\Delta H^{\ddagger}$ and $\Delta S^{\ddagger}$ without influencing noticeably $\Delta G^{\ddagger}$.

We can study the experimental trends by introducing a solvent dependence on $\Delta S^{\ddagger}$ in addition to that already considered for $\Delta H^{\ddagger}$ through the electrostatic solvation interaction[34] $\Delta H^{\ddagger el}(s)$, Table 1. The entropy of activation $\Delta S^{\ddagger}$ is negative, in Table 1, because two molecules (CH_3I and **1**) are brought together to form one single species **TS[1−2]** under the loss of both translational and rotational entropy. However, our estimate of the loss ($\Delta S^{\ddagger}(s)$) is exaggerated concerning freedom in both translation and rotation. The loss is likely smaller in real solution, where both motions to some degree are hindered.

The contribution to $\Delta H^{\ddagger}$ from the electrostatic solvation term $\Delta H^{\ddagger el}(s)$ is negative and largely due to a stabilization of the polar transition state where I^- is at the verge of dissociating, as shown in Table 1 and Figure 1.

The coordinatively unsaturated low-spin d^6 methyl complex $[M(CO)_2I_2(CH_3)]$ (M = Rh, Ir) resulting from the complete dissociation of iodide in the oxidative addition process adopts a square pyramidal conformation with CH_3 in the apical position. According to simulations based on ab initio molecular dynamics (AIMD), which was done in our group for this system but was not included in this paper, before the complex can adopt other conformations, the iodide ion can attack the empty coordination site.

Table 2. Computed Reaction Thermodynamics[a] for the Formation of $[M(CO)_2I_3(CH_3)]^-$ from $[M(CO)_2I_2]^-$

M	ΔS(g)[c]	ΔH(g)[c]	ΔG(g)[c]	ΔH(s)[b,d]	ΔG(s)[b,e]
Rh	−43.0	−6.8	6.0	−5.0	7.9
Ir	−42.7	−16.6	−3.9	−14.7	−2.0

[a] Reaction eq 1 in the text. All energies are in kcal mol^{-1}, entropies in cal K^{-1} mol^{-1}. [b] Solvent is methanol. [c] ΔS(g), ΔH(g), and ΔG(g) are ΔS, ΔH, and ΔG from gas phase calculations. [d] $\Delta H(s) = \Delta H(g) + \Delta H^{el}(s)$. Here $\Delta H^{el}(s)$ is the electrostatic solvation stabilization (see ref 34) calculated after static calculation. [e] $\Delta G(s) = \Delta H(s) - T\Delta S(g)$.

Table 3. Computed Reaction Thermodynamics[a] for the Formation of $[M(CO)L_2I(CH_3)]^{(n-1)-}$ from $[M(CO)L_2I]^{n-}$

M	L_2	ΔS(g)[c]	ΔH(g)[c]	ΔG(g)[c]	ΔH(s)[b,d]	ΔG(s)[b,e]
Rh	$(CO)I^-$	−14.5	31.8	36.2	7.5	11.8
	trans-$(PEt_3)_2$	−2.4	93.9	94.6	1.8	2.5
	$Ph_2PCH_2CH_2PPh_2$	−14.6	89.2	93.5	4.3	8.7
	$Ph_2PCH_2P(S)Ph_2$	−14.9	84.0	88.4	1.3	5.7
	(*S,P*-$SC_2B_{10}H_{10}PPh_2)^-$	−11.4	24.0	27.5	−2.1	1.3
Ir	$(CO)I^-$	−11.9	26.3	29.8	2.0	5.6
	$(CO)_2$	−14.3	129.9	134.1	19.8	24.0
	(CO)(Sol)[b]	−13.5[f]			9.5	13.5[f]

[a] Reaction eq 2 in the text. All energies are in kcal mol^{-1}, entropies in cal K^{-1} mol^{-1}. [b] Solvent is methanol. [c] ΔS(g), ΔH(g), and ΔG(g) are ΔS, ΔH, and ΔG from gas phase calculations. [d] $\Delta H(s) = \Delta H(g) + \Delta H^{el}(s)$. Here $\Delta H^{el}(s)$ is the electrostatic solvation stabilization (see ref 34) calculated after static calculation. [e] $\Delta G(s) = \Delta H(s) - T\Delta S(g)$. [f] $\Delta S(s)$ was calculated for this complex. Therefore, $\Delta G(s) = \Delta H(s) - T\Delta S(s)$.

We find that the oxidative addition reaction (**1** → **2**) is exergonic for iridium and endergonic for rhodium, as shown in Table 2. This trend reflects the relativistic stabilization of the Ir−CH_3 bond relative to the Rh−CH_3 linkage. Experimental data[8b] are available for rhodium with $\Delta G = 3.2$ kcal mol^{-1} compared to our calculated value of 7.9 kcal mol^{-1}.

2. Relation between Ancillary Ligands (L_2) and Heat of Reaction for Nucleophilic Attack by $[M(CO)L_2I]^{n-}$ (M = Rh, Ir; *n* = 0 or 1) on CH_3I. The rate-determining step in the oxidative addition process of eq 1 was the nucleophilic attack of CH_3I by $[M(CO)_2I_2]^-$. We have studied how different ancillary ligands (L_2) influence the heat of reaction for this S_N2 process further by considering the thermochemistry for

$$[M(CO)L_2I]^{n-} + CH_3I \rightarrow [M(CO)L_2I(CH_3)]^{(n-1)-} + I^- \quad (n = 0 \text{ or } 1) \quad (2)$$

with L_2 = $(CO)I^-$, *trans*-$(PEt_3)_2$, $Ph_2PCH_2CH_2PPh_2$ (dppe), $Ph_2PCH_2P(S)Ph_2$ (dppms), or *S,P*-$SC_2B_{10}H_{10}PPh_2^-$ for M = Rh and L_2 = $(CO)I^-$, $(CO)_2$, or (CO)(MeOH) for M = Ir; see Table 3.

During the oxidative addition the M−CH_3 and CH_3−I distances vary more appreciably than any other bond length. The M−CH_3 bond lengths decrease from far apart in **1** to 2.19−2.21 Å in adduct **A[1−2]** and to 2.12−2.14 Å in **TS[1−2]** (see Tables 4, 5 and Figure 1), whereas the CH_3−I distances increase from 2.22 Å to 3.15−3.36 Å in adduct **A[1−2]** and to 4.92−5.36 Å in **TS[1−2]**. In case of iridium, the breakage of the CH_3−I

(38) Ziegler, T.; Tschinke, V.; Ursenbach, C. *J. Am. Chem. Soc.* **1987**, *109*, 4825.
(39) Connors, K. A. *Chemical Kinetics: The Study of Reaction Rates in Solution*; VCH: New York, 1990.
(40) (a) Boudart, M.; Djega-Mariadassou, G. *Kinetics of Heterogeneous Catalytic Reactions*; Princeton University Press: Princeton, 1984. (b) Linert, W.; Kadrjawtsev, A. B. *Aust. J. Chem.* **1984**, *37*, 1139. (c) Linert, W.; Kadrjawtsev, A. B.; Schmid, R. *Aust. J. Chem.* **1983**, *36*, 1903. (d) Linert, W.; Jameson, R. F. *CSRVBR* **1989**, *18*, 477. (e) Exner, O. *Collect. Czech. Chem. Commun.* **1974**, *24*, 514. (f) Linert, W. *Chem. Soc. Rev.* **1994**, *23*, 429.

Table 4. Optimized Bond Distances[a] in the Reactants (1), Adducts (A[1−2]), Transition States (TS[1−2]), and $CH_3-M(CO)_2I_2$ for the Oxidative Addition of Methyl Iodide

	reactant			adduct				transition state				$CH_3-M(CO)_2I_2$
	M−CO	M−I	I−CH_3	M−CH_3	I−CH_3	M−CO	M−I	M−CH_3	I−CH_3	M−CO	M−I	M−CH_3
cis-$[Rh(CO)_2I_2]^-$	1.84	2.77	2.22	2.21	3.15	1.88	2.75	2.12	4.92	1.89	2.73	2.11
cis-$[Ir(CO)_2I_2]^-$	1.84	2.78	2.22	2.19	3.36	1.87	2.76	2.14	5.36	1.88	2.75	2.14

[a] Distances are in Å.

Table 5. Optimized Bond Angles[a] in the Reactants (1), Adducts (A[1−2]), Transition States (TS[1−2]), and $CH_3-M(CO)_2I_2$ for the Oxidative Addition of Methyl Iodide

	reactant	adduct			transition state		$CH_3-M(CO)_2I_2$
	H−C−I	M−C−H	M−C−I	H−C−I	M−C−H	M−C−I	M−C−H
cis-$[Rh(CO)_2I_2]^-$	107.1	102.8	175.9	77.2	105.9	101.5	106.5
cis-$[Ir(CO)_2I_2]^-$	107.1	105.4	176.8	74.6	106.7	174.4	107.3

[a] Angles are in degrees.

bond in the transition state has proceeded appreciably. On the other hand, the M−CO bonds increase by 0.04−0.05 Å and M−I bonds decrease by 0.03−0.04 Å, which is a small change in bond distances. This underlines that the reaction primarily involves the formation of the M−CH_3 bond in the adduct-forming stage followed by the fission of the CH_3−I bond in the transition state.

We also note the bending of the M−C−I angle in the case of rhodium in Table 5. However, this change does not have much effect on the reaction rate, as the energy barrier for this bending is quite small. The M−C−H angle increases as the reaction proceeds, while the H−C−I angle decreases. The M−C−H angle in the transition state is almost the same as that in Me-$M(CO)_2I_2$.

As can be seen in the structures in Table 4, the M−CH_3 bond distance in the transition state is very close to those in Me−$M(CO)_2I_2$, which might be the intermediate in the reaction process before iodide attacks it to produce the final product. This is indicative of a late transition state. Therefore, comparing the energy difference between the intermediate $[M(CO)L_2I(CH_3)]^{(n-1)-}$ and the reactant $[M(CO)L_2I]^{n-}$ might give important information on the reaction rate.

The most direct influence of the ancillary ligands L on the energetics of the nucleophilic attack in eq 2 is through their ability to increase the nucleophilicity and electron density of the metal complex and thus facilitate the attack on methyl iodide. For $L_2 = (CO)I^-$, the difference in ΔG(s) for the reaction in eq 2 between rhodium and iridium is 6.2 kcal/mol, as shown in Table 3. This difference is quite comparable to the difference in $\Delta G^{\ddagger}$(s) (7.6 kcal/mol) between the two metals for the same process. This is understandable since the nucleophilic attack has a late transition state **TS[1−2]**, Figure 1, with considerable C−I bond breaking.

For all ligand combinations the S_N2 process is seen to have slightly negative reaction entropy, Table 3. We can understand this by observing that the rotational entropy lost by CH_3I is not gained again by the dissociation of I^-. Further, the S_N2 reaction is in general endothermic in the gas phase. This is especially the case for $n = 0$, where the dissociation of I^- corresponds to a charge separation in which a cation is left behind. This charge effect is neutralized in solution, but the S_N2 reaction is still endothermic, except for *S,P*-$SC_2B_{10}H_{10}PPh_2^-$, Table 3. It follows finally from the calculated ΔG(s) values that the process in general is endergonic with free energies of reaction that follows the order $(CO)_2$ > (CO)(solvent) > $(CO)(I^-)$ > dppe > dppms > *trans*-$(PEt_3)_2$ > *S,P*-$SC_2B_{10}H_{10}PPh_2^-$.

With respect to the individual ligand combinations we note that $[M(CO)_3I]$ ($L_2 = (CO)_2$) has been known to be unreactive. This is not surprising since the three carbonyl ligands make the metal center electron poor and thus unable it to exhibit any nucleophilic behavior.[12] In fact, we calculate ΔG(s) to be 24.0 kcal mol^{-1} for the nucleophilic attack on CH_3I by $[M(CO)_3I]$, which is the highest number among the different ligand combinations. Further, $[M(CO)_3I]$ was found to be the major species in a media with low levels of water and ionic iodide. Finally, the presence of $[Ir(CO)_3I]$ was thought to be the reason for the low activities of iridium complexes under high CO pressure. On the other hand, prior dissociation of one of the carbonyl ligands under lower CO pressure produces $[M(CO)_2(solvent)I]$, which is capable of a rather slow oxidative addition reaction. We calculate ΔG(s) for the nucleophilic attack involving $[Ir(CO)_2I(solvent)]$ to be 13.5 kcal mol^{-1}, which is the next highest number calculated for the different ligand combinations, Table 3.

$Rh(CO)L_2(I)$ with L_2 = dppe, dppms, and *trans*-$(PEt_3)_2$ all have lower reaction enthalpies (ΔH(s)) and free energy of reaction (ΔG(s)) in solution with respect to the nucleophilic attack on CH_3I in solution than $[Rh(CO)_2I_2]^-$, Table 3. This is to be expected on account of the larger donor ability of the phosphine ligands in comparison with the $L_2 = (CO)(I^-)$ combination. Also for the case of $n = 0$, the facile solvation of the intermediate $[M(CO)L_2I(CH_3)]^+$ compared to the reactant $[M(CO)L_2I]$ seems to be very important in polar solvent. Indeed experiment[18,19] seems to indicate that the three phosphines are excellent candidates for boosting the nucleophilicity of the rhodium center toward CH_3I. The most interesting ligand is *S,P*-$SC_2B_{10}H_{10}PPh_2^-$. When this ligand is coordinated to Rh, the nucleopilicity of $Rh(CO)L_2(I)$ toward CH_3I is larger than for $[Rh(CO)_2I_2]^-$ (Table 3), having the lowest reaction enthalpies (ΔH(s)) and free energy of reaction (ΔG(s)) in solution. Therefore, we propose that by using various anionic phosphine ligands we might be able to obtain a catalyst with increased activities.

Concluding Remarks

We have carried out quantum mechanical calculations based on density functional theory (DFT) on the oxida-

tive addition process $[M(CO)_2I_2]^- + CH_3I \rightarrow [M(CO)_2I_3(CH_3)]^-$ (M = Rh, Ir).

The calculated free energies of activation ($\Delta G^{\ddagger}$) in methanol are 19.3 (Ir) and 26.9 kcal mol^{-1} (Rh), respectively, in good agreement with the experimental estimates at 20.9 kcal mol^{-1} (Ir) in dichloromethane and 22.9 kcal mol^{-1} (Rh) in methanol, respectively. The higher barrier for M = Rh is attributed to a relativistic stabilization of the Ir−CH_3 bond.

A thermodynamic calculation was carried out on the formation of the intermediate $[M(CO)L_2ICH_3]^{(n-1)-}$ in the general oxidative addition reaction $[M(CO)L_2I]^{n-} + CH_3I \rightarrow [M(CO)L_2ICH_3]^{(n-1)-} + I^-$ (n = 0 or 1) (where L_2 = (CO)I^-, $(CO)_2$, or (CO)(MeOH) for M = Ir and L_2 = (CO)I^-, *trans*-$(PEt_3)_2$, $Ph_2PCH_2CH_2PPh_2$, $Ph_2PCH_2P(S)Ph_2$, or *S,P*-$SC_2B_{10}H_{10}PPh_2^-$ for M = Rh). The thermodynamic energy difference between the intermediate $[M(CO)L_2ICH_3]^{(n-1)-}$ and the ground state follows the order *S,P*-$SC_2B_{10}H_{10}PPh_2^-$ < *trans*-$(PEt_3)_2$ < $Ph_2PCH_2P(S)Ph_2$ < $Ph_2PCH_2CH_2PPh_2$ < (CO)I^- < $(CO)_2$ in solution with respect to the ligand L_2. This order is to a first approximation determined by the ability of L to stabilize the M−CH_3 bond being formed and the ability of the solvent to stabilize the intermediate $[M(CO)L_2ICH_3]^{(n-1)-}$ relative to the ground state. This order agrees well with the experimental kinetic trend. Therefore, a simple thermodynamic calculation can be used to predict the activity of a catalyst and to propose a possible candidate for a good catalyst.

Acknowledgment. M.C. is pleased to acknowledge financial support by Kyung Hee University in building a linux cluster for ADF calculations. This work has been partially supported by the National Science and Engineering Research Council of Canada (NSERC).

Supporting Information Available: Optimized geometries of the crucial structures reported (Cartesian coordinates, in Å). This material is available free of charge via the Internet at http://pubs.acs.org.

OM049383Q